

Antiproliferative Evaluation of Some 2-[2-(2-Phenylethenyl)cyclopent-3-en-1-yl]-1,3-benzothiazoles: DFT and Molecular Docking Study

Mustafa Ceylan,^{*a} Sultan Erkan,^b Ayse Sahin Yaglioglu,^c Nuray Akdogan Uremis,^a and Esra Koç^a

^a Department of Chemistry, Tokat Gaziosmanpaşa University, 60250 Tokat, Turkey,
e-mail: mustafac.ceylan@gop.edu.tr

^b Department of Chemistry and Chemical Process Technology, Sivas Cumhuriyet University, 58140 Sivas, Turkey

^c Department of Chemistry, Faculty of Science, Çankırı Karatekin University, 18100 Çankırı, Turkey

The 2-[2-(2-phenylethenyl)cyclopent-3-en-1-yl]-1,3-benzothiazoles were synthesized from the reactions of 7-benzylidenebicyclo[3.2.0]hept-2-en-6-ones with 2-aminobenzenethiol. The antiproliferative activities of 2-[2-(2-phenylethenyl)cyclopent-3-en-1-yl]-1,3-benzothiazoles were determined against C6 (rat brain tumor) and HeLa (human cervical carcinoma cells) cell lines using BrdU cell proliferation ELISA assay. Cisplatin and 5-fluorouracil (5-FU) were used as standards. The most active compound was 2-[(1S,2S)-2-[(E)-2-(4-methylphenyl)ethenyl]cyclopent-3-en-1-yl]-1,3-benzothiazole against C6 cell lines with $IC_{50} = 5.89 \mu\text{M}$ value (cisplatin, $IC_{50} = 14.46 \mu\text{M}$ and 5-FU, $IC_{50} = 76.74 \mu\text{M}$). Furthermore, the most active compound was 2-[(1S,2S)-2-[(E)-2-(2-methoxyphenyl)ethenyl]cyclopent-3-en-1-yl]-1,3-benzothiazole against HeLa cell lines with $IC_{50} = 3.98 \mu\text{M}$ (cisplatin, $IC_{50} = 37.95 \mu\text{M}$ and 5-FU, $IC_{50} = 46.32 \mu\text{M}$).

Additionally, computational studies of related molecules were performed by using B3LYP/6-31G+(d,p) level in the gas phase. Experimental IR and NMR data were compared with the calculated results and were found to be compatible with each other. Molecular electrostatic potential (MEP) maps of the most active 2-[(1S,2S)-2-[(E)-2-(2-methoxyphenyl)ethenyl]cyclopent-3-en-1-yl]-1,3-benzothiazole against HeLa and the most active 2-[(1S,2S)-2-[(E)-2-(4-methylphenyl)ethenyl]cyclopent-3-en-1-yl]-1,3-benzothiazole against C6 were investigated, aiming to determine the region that the molecule is biologically active. Biological activities of mentioned molecules were investigated with molecular docking analyses. The appropriate target protein (PDB codes: 1 M17 for the HeLa cells and 1JQH for the C6 cells) was used for 2-[(1S,2S)-2-[(E)-2-(2-methoxyphenyl)ethenyl]cyclopent-3-en-1-yl]-1,3-benzothiazole and 2-[(1S,2S)-2-[(E)-2-(4-methylphenyl)ethenyl]cyclopent-3-en-1-yl]-1,3-benzothiazole molecules exhibiting the highest biological activity against HeLa and C6 cells in the docking studies. As a result, it was determined that these molecules are the best candidates for the anticancer drug.

Keywords: 2-[2-(2-phenylethenyl)cyclopent-3-en-1-yl]-1,3-benzothiazole, antiproliferative activity, HeLa, C6, 5-fluorouracil, computational study.

Introduction

Benzothiazole derivatives are an important class of heterocyclic compounds possessing a wide range of biological activities and are therefore of great interest for bioorganic and medicinal chemists.^[1,2] The benzothiazole derivatives show promising anticancer^[3,4] activities. The 2-arylbenzothiazoles have been used as anticancer agents.^[5] For example, substituted benzothiazole PMX 610 (2-(3,4-dimethoxyphenyl)-5-fluoro-

benzothiazole, *Figure 1*) was shown to exhibit exquisitely potent ($GI_{50} < 0.1 \text{ nM}$) and to have *in vitro* antitumor properties against sixty human cancer cells (e.g., colon, non-small-cell lung and breast subpanels) in the National Cancer Institute (NCI).^[6] The fluorinated benzothiazoles A and B (*Figure 1*) exhibited the best activity against MCF-cell lines with GI_{50} values of 0.57 and 0.4 μM , respectively.^[7]

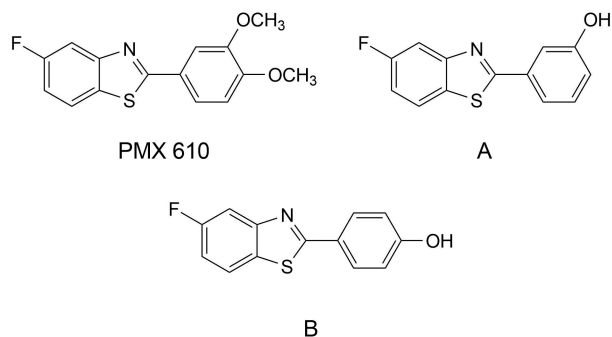


Figure 1. The structures of PMX 610 and the fluorinated benzothiazoles A and B.

Moreover, 2-aminobenzothiazoles exhibit cytotoxic activity against several types of carcinoma cells.^[8] Further investigation led to the identification of 2-(4-aminophenyl)benzothiazoles as the promising and selective antitumor agents.^[9]

Although numerous benzothiazole derivatives included 2-amino- and 2-arylbenzothiazoles have been investigated as antitumor agents,^[10–12] there are a limited number of researches on 2-alkylsubstituted benzothiazoles.

Recently, we reported^[13] the *in vitro* cytotoxic evaluation of some *cis*-substituted 1,3-benzothiazole derivatives against HeLa (Human Cervical Carcinoma Cells) and C6 (Rat Brain Tumor) cancer cells. Compounds showed high activity with IC_{50} values ranging from $IC_{50} \leq 5 \mu\text{M}$ to $IC_{50} = 9.53 \mu\text{M}$ compared to 5-FU ($IC_{50} \leq 5 \mu\text{M}$). In another research of ours,^[14] we investigated the antiproliferative activity of 2-styrylcyclopentyl substituted 1,3-benzothiazole derivatives against PANC-1 pancreatic cancer cells and demonstrated that compounds (with IC_{50} of $27 \pm 0.24 \mu\text{M}$ and $35 \pm 0.51 \mu\text{M}$) had much higher cytotoxicity on the PANC-1 pancreatic cancer cell lines compare to gemcitabine (IC_{50} of $52 \pm 0.72 \mu\text{M}$).

Thus, in this article, we focused on the synthesis of 2-alkylsubstituted benzothiazole derivatives, 2-[2-(2-phenylethenyl)cyclopent-3-en-1-yl]-1,3-benzothiazoles **5a–5m**, and evaluation of their antiproliferative activities against HeLa (Human Cervical Cancer Cells) and C6 (Rat Brain Tumor) cancer cells.

Additionally, in recent years, computational chemistry has become a field of reference for elucidating the structure and determining the biological activity of molecules.^[15–20] Nowadays, computational chemistry methods are used to investigate the properties of drug substances. These methods reduce the cost of production and prevent time loss. The proper-

ties and activity areas of the molecules with computational chemistry methods are computed and simulated with the help of a computer. The information obtained by the experimental methods used to determine the molecular structure could be used in computational chemistry methods to design new drug molecules or to further develop existing drugs.^[21]

Compounds **5a–5m** are optimized at DFT/B3LYP/6-31G+(d,p) level in the gas phase. The computed and experimentally observed spectroscopic values were examined on 5j–5m to give a detailed assignment of the fundamental bands in FT-IR and NMR. Comparisons and labeling showed that the calculation results and the experimental data were quite compatible with each other. This compatibility obtained from the spectroscopic data shows that the selected B3LYP/6-31G+(d,p) level for the calculation is an appropriate level and is a level that can be used for all other calculations. The chemical activity areas of the studied compounds are determined via Molecular Electrostatic Potential (MEP) maps. In this study, MEP maps were investigated for two compounds **5c** and **5e** with high activity against two cell lines, and the reactive regions of these molecules were determined. In recent years, molecular docking studies have drawn attention to their biological reactivity studies. Molecular docking simulation plays an important role in drug design and is used to predict binding forces and biological activities between drug molecules and their protein receptors.^[22] The molecules of compounds **5c** and **5e** that are active against the two cell lines were docked with the target proteins corresponding to the cancer cells which are examined. Then, the interaction energies and binding mode were investigated. The binding energies of HeLa and C6 cells with the molecules of **5c** and **5e** showing high inhibitory activity were investigated.

Results and Discussion

Chemistry

The 7-benzylidenebicyclo[3.2.0]hept-2-en-6-ones **3a–3m** were synthesized from the condensation of substituted benzaldehyde derivatives **2a–2m** with (1*R*,5*S*)-bicyclo[3.2.0]hept-2-en-6-one (**1**), which was commercially available in the basic form according to the previously published method.^[23] The compounds **3a–3i** are known and the compounds **3j–3m** were synthesized for the first time in this study. Compounds **3a–3m** were put in reaction with 2-aminobenzethiol (**4**) in the presence of TsOH to get the 2-[2-(2-

phenylethenyl)cyclopent-3-en-1-yl]-1,3-benzothiazoles (**5a–5m**). The reaction was carried out according to the reported method^[24] and the compounds **5a–5m** were obtained in high yields of 91–98% (Scheme 1 and Table 1). In addition, compounds **5j–5m** are novel, while the others are already known. The structures of all compounds were elucidated by spectroscopic methods (IR, NMR) together with elemental analysis and comparison with literature data. All physical and spectroscopic data are in accordance with the proposed structures.^[23,24]

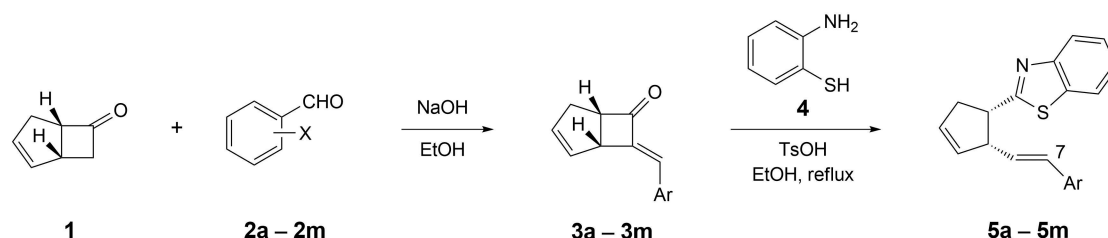
Antiproliferative Activity

The antiproliferative activities of compounds **5a–5m** were determined against C6 and HeLa cell lines using BrdU cell proliferation ELISA assay.^[25,26] The compounds, cisplatin and 5-FU were dissolved in DMSO. Then, each sample was diluted with DMEM. At the final concentrations, DMSO was below 1%. The cells were incubated for 24 h at 37 °C in a humidified atmosphere of 5% CO₂. Cultured cells were grown in 96-well plates (COSTAR, Corning, USA) at a density of 3 × 10⁴ cells well. Results were reported as percentage of the inhibition of cell proliferation, where the optical density measured from vehicle-treated cells was 100%

of proliferation. All assays were repeated at least twice using HeLa and C6 cell lines. Percentage of inhibition of cell proliferation was calculated as follows: $[1 - (A_{\text{samples}}/A_{\text{control}})] \times 100$.

The experiments were done three times ($n = 9$). The antiproliferative activities of **5a–5m** and the controls were investigated on 5, 10, 20, 30, 40, 50, 75 and 100 μm concentrations, and cisplatin and 5-fluorouracil were used as standards. The results are given as the IC₅₀ values in Table 2.

According to Table 2, the compound **5e** has the highest antiproliferative activity against the C6 cell lines. In addition, this molecule exhibits a very high inhibitory activity relative to cisplatin and 5-FU. As shown in Table 1, the compound **5f** has significantly higher antiproliferative activity than cisplatin and 5-FU. While the other compounds have higher activity than 5-FU, they have lower activity than cisplatin. When the antiproliferative activity of the compounds **5a–5m** against HeLa cell lines is examined, it appears that the most active compounds are **5c** and **5g**. The compounds **5a, 5b, 5i, 5j** and **5l** have considerably higher activity than both cisplatin and 5-FU. As a result, the studied serial molecules may be very useful in terms of antiproliferative activity.



Scheme 1. Synthesis of the 2-[2-(2-phenylethenyl)cyclopent-3-en-1-yl]-1,3-benzothiazoles **5a–5m**.

Table 1. Synthesis of 2-[2-(2-phenylethenyl)cyclopent-3-en-1-yl]-1,3-benzothiazoles **5a–5m**.

Entry	3	Yield [%]	Ar	5	Yield [%]
1	3a	97	4-MeO-C ₆ H ₄	5a	97
2	3b	96	4-Cl-C ₆ H ₄	5b	96
3	3c	95	2-MeO-C ₆ H ₄	5c	93
4	3d	94	2-Br-C ₆ H ₄	5d	98
5	3e	93	4-Me-C ₆ H ₄	5e	97
6	3f	91	2-thiophenyl	5f	97
7	3g	92	2-furyl	5g	93
8	3h	94	3-Br	5h	95
9	3i	91	3-Me-C ₆ H ₄	5i	97
10	3j	97	4-Br-C ₆ H ₄	5j	98
11	3k	98	4-F-C ₆ H ₄	5k	92
12	3l	87	2,5-Cl ₂ -C ₆ H ₃	5l	94
13	3m	81	4-NO ₂ -C ₆ H ₄	5m	91

Table 2. IC₅₀ values (μM) of compounds **5a–5m** against C6 and HeLa (*n* = 9).

Compounds	C6	HeLa
5a	38.24 ± 0.05	14.72 ± 0.05
5b	48.10 ± 0.02	16.37 ± 0.02
5c	69.98 ± 0.05	3.98 ± 0.05
5d	40.11 ± 0.02	77.89 ± 0.05
5e	5.89 ± 0.02	44.27 ± 0.05
5f	13.17 ± 0.01	82.35 ± 0.02
5g	35.92 ± 0.05	6.19 ± 0.02
5h	31.68 ± 0.01	45.39 ± 0.05
5i	73.92 ± 0.01	25.27 ± 0.01
5j	23.12 ± 0.05	11.01 ± 0.01
5k	32.16 ± 0.01	54.10 ± 0.05
5l	14.59 ± 0.05	20.60 ± 0.05
5m	35.57 ± 0.02	46.82 ± 0.02
Cisplatin	14.46 ± 0.05	37.95 ± 0.02
5-FU	76.74 ± 0.02	46.32 ± 0.05

Against the HeLa cell lines, the methoxy group in molecules **5a** and **5c** enhances the activity of the phenyl ring as the *ortho* and *para* promoter. Activity is also increased accordingly. Against the C6 cell lines, the methyl group in molecule **5e** increases the activity of the phenyl ring as the *ortho* and *para* promoter, thereby increasing the activity.

Optimized Structures

Mentioned compounds were optimized at B3LYP/6-31G+(d,p) level in the gas phase. Optimized structures of related molecules are represented in *Figure 2*.

IR Spectrum of Ligands

DFT offers significant advantages in predicting harmonic vibrational force fields, frequencies, and spectra.^[27] The harmonic frequencies obtained by DFT calculations are multiplied by a scale factor in the literature to obtain harmonic frequencies. The scale factor for B3LYP/6-31G+(d,p) level is 0.9640.^[28] Experimental IR spectra (KBr, ν_{max} cm⁻¹) and calculated frequencies at B3LYP/6-31G+(d,p) level in the gas phase of the studied molecules are given in *Table 3*.

For the compounds **5j–5m**, the correlation coefficients (R²) between experimental and calculated vibrational frequencies were determined. These coefficients for **5j–5m** are 0.9975, 0.9963, 0.9982 and 0.9986, respectively. According to R² values, it implies that closer value to 1 is the more real structure.^[29] All these R² values are close to 1. In this case, it could be said that the optimized structures and the experimen-

tal structures are compatible with each other. Experimental frequencies, calculated frequencies and related assignment are shown in *Table 3*. The experimental frequencies were labeled with the corresponding vibration mode types with the aid of a given animation program. According to *Table 3*, the experimental frequency in 3056 cm⁻¹ was calculated as 3068.8 cm⁻¹ and this stretching was labeled C–H bond stretching in the benzene ring for **5j**. The frequency for the 2929 cm⁻¹ experimental frequency was calculated as 2953.5 cm⁻¹ and the calculated frequency was labeled to the C–H stretching at the cyclopent-3-enyl. For the **5j** molecule, the experimental frequency at 2850 cm⁻¹ was calculated as 2939.1 cm⁻¹, and it was seen that this vibration frequency was the C–H vibration in aliphatic CH=CH. The frequency experimentally at 1590 cm⁻¹ corresponded to the frequency at 1603.9 cm⁻¹ from the calculated frequencies, and this frequency was labeled as C=C stretching at the cyclopent-3-enyl, aliphatic C=C and aromatic C=C stretching. The experimental frequency at 1436 cm⁻¹ was calculated as 1521.6 cm⁻¹, and it was seen that this frequency corresponds to N=C bond stretching. The experimental frequency at 1311 cm⁻¹ and this frequency was calculated as 1471.5 cm⁻¹ and labeled as C–C in the benzene ring and as C–H rocking. This time, the experimental frequency for symmetric C–N bond stretching and C–H rocking is 1241 cm⁻¹ while the calculated frequency is 1263.5 cm⁻¹. The experimental frequency at 1108 cm⁻¹ corresponded to the calculated frequency at 1139.8 cm⁻¹ and this frequency was labeled C–C stretching. The experimental frequency at 964 cm⁻¹ was calculated as 983.8 cm⁻¹ and the corresponding vibration mode of this frequency was labeled as C–Br bond stretching. The experimental frequency at 759, 728 and 682 cm⁻¹ was calculated as 808.9, 742.3 and 709.5 cm⁻¹, respectively, and this frequency labeled as wagging^[30] in hydrogens attached to the aromatic carbon. The similar data were obtained for other compounds. As a result, the experimental parameters and the calculated frequencies are very close to each other. Thanks to this harmonization, accurate predictions can be made in this study with computational chemistry methods.

¹H-NMR of Ligands

One of the methods used for structural characterization is nuclear magnetic resonance (NMR) spectroscopy. Nowadays, ¹H- and ¹³C-NMR analyses are mainly used in the building lighting. By means of computational chemistry methods, chemical shift values are

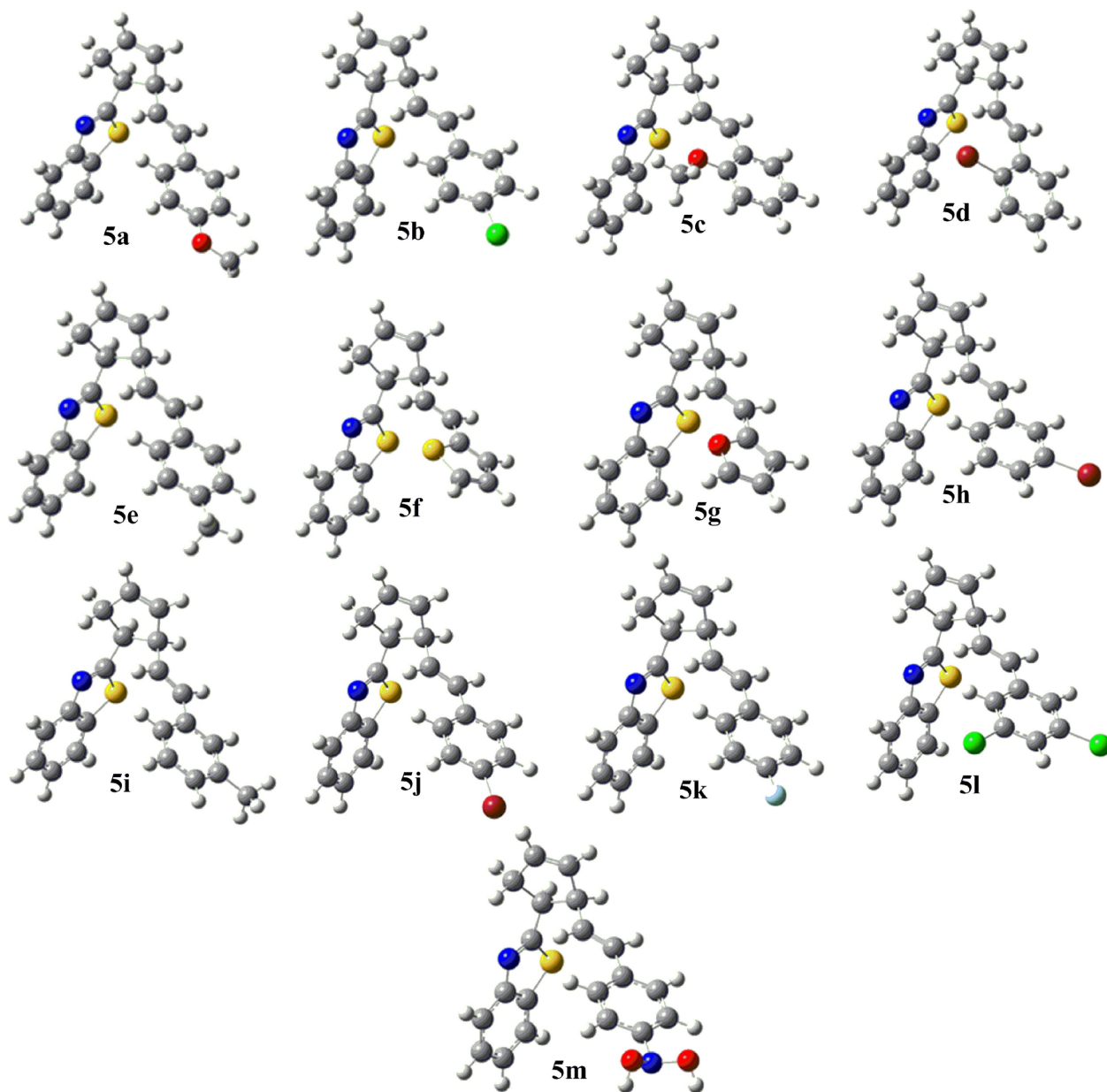


Figure 2. Optimized structures of compounds **5a–5m** at B3LYP/6-31G+(d,p) level.

obtained for all of the atoms in the molecule. ^1H - and ^{13}C -NMR analyses were carried out at the level of B3LYP/6-31G+(d,p) in the gas phase by using GIAO method for the compounds studied. The experimental ^1H -NMR data for studied molecules were given in the *Experimental Section*.

Atomic labeling of **5j–5m** molecules for ^1H -NMR data calculated at GIAO method in B3LYP/6-31g+(d,p) level are given in *Figure 3*. Calculated proton and carbon chemical shift values are presented in *Table 4*.

The chemical shift value for H3 in the **5j** molecule is 8.77 ppm. This value is the highest chemical shift value found in the **5j** molecule. This data may correspond to the 8.01 ppm chemical shift found experimentally. The chemical shift value calculated as 8.43 ppm for H4 in this molecule may correspond to experimental 7.87 ppm chemical shift value.

The calculations show that the chemical shift values for H_2O and H2 are 8.19 and 8.03 ppm, respectively. These values correspond to the experimental chemical shifts of 7.57 and 7.52–7.45 ppm, respectively. When

Table 3. Some experimental and calculated frequencies (cm^{-1}) of mentioned ligand at B3LYP/6-31G + (d,p) level in gas phase.^[a]

5j			5k		
Exp.	Calc.	Assign.	Exp.	Calc.	Assign.
3056	3068.8	$\nu_{\text{C}_{\text{aro}}-\text{H}}$	3056	3092.8	$\nu_{\text{C}_{\text{aro}}-\text{H}}$
2929	2953.5	$\nu_{\text{C}-\text{H}_{\text{cyclopent-3-enyl}}}$	2962	3080.7	$\nu_{\text{C}-\text{H}_{\text{cyclopent-3-enyl}}}$
2850	2939.1	$\nu_{\text{C}_{\text{ali}}-\text{H}}$	2850	2938.7	$\nu_{\text{C}_{\text{ali}}-\text{H}}$
1590	1603.9	$\nu_{\text{C}-\text{C}_{\text{cyclopent-3-enyl}}} + \nu_{\text{C}_{\text{ali}}=\text{C}_{\text{ali}}} + \nu_{\text{C}_{\text{aro}}-\text{C}_{\text{aro}}}$	1646	1607.5	$\nu_{\text{C}-\text{C}_{\text{cyclopent-3-enyl}}} + \nu_{\text{C}_{\text{ali}}=\text{C}_{\text{ali}}} + \nu_{\text{C}_{\text{aro}}-\text{C}_{\text{aro}}}$
1436	1521.6	$\nu_{\text{N}=\text{C}}$	1509	1522.1	$\nu_{\text{N}=\text{C}}$
1311	1471.5	$\nu_{\text{C}_{\text{aro}}-\text{C}_{\text{aro}}} + \delta_{\text{C}_{\text{aro}}-\text{H}}$	1436	1488.9	$\nu_{\text{C}_{\text{aro}}-\text{C}_{\text{aro}}}$
1241	1263.5	$\nu_{\text{C}-\text{N}} + \delta_{\text{C}_{\text{aro}}-\text{H}}$	1261	1263.6	$\nu_{\text{C}-\text{N}}$
1108	1139.8	$\nu_{\text{C}-\text{C}}$	1091	1097.6	$\nu_{\text{C}-\text{C}}$
964	983.8	$\nu_{\text{C}-\text{Br}}$	1012	1037.1	$\nu_{\text{C}-\text{S}}$
759	808.9	$\omega_{\text{C}_{\text{aro}}-\text{H}}$	802	955.6	$\omega_{\text{C}_{\text{aro}}-\text{H}}$
728	742.3	$\omega_{\text{C}_{\text{aro}}-\text{H}}$	727	766.3	$\nu_{\text{C}_{\text{aro}}-\text{F}}$
682	709.5	$\omega_{\text{C}_{\text{aro}}-\text{H}}$			

5l			5m		
Exp.	Calc.	Assign.	Exp.	Calc.	Assign.
3056	3093.1	$\nu_{\text{C}_{\text{aro}}-\text{H}}$	3064	3093.2	$\nu_{\text{C}_{\text{aro}}-\text{H}}$
2962	3047.3	$\nu_{\text{C}_{\text{ali}}-\text{H}}$	2971	3036.3	$\nu_{\text{C}_{\text{ali}}-\text{H}}$
2850	2955.7	$\nu_{\text{C}-\text{H}_{\text{cyclopent-3-enyl}}}$	2940	2950.5	$\nu_{\text{C}-\text{H}_{\text{cyclopent-3-enyl}}}$
1646	1603.7	$\nu_{\text{C}-\text{C}_{\text{cyclopent-3-enyl}}} + \nu_{\text{C}_{\text{ali}}=\text{C}_{\text{ali}}} + \nu_{\text{C}_{\text{aro}}-\text{C}_{\text{aro}}}$	2865	2918.9	$\nu_{\text{C}_{\text{ali}}-\text{H}}$
1509	1538.7	$\nu_{\text{C}_{\text{aro}}-\text{C}_{\text{aro}}}$	1635	1602.0	$\nu_{\text{C}=\text{C}_{\text{cyclopent-3-enyl}}} + \nu_{\text{C}_{\text{ali}}=\text{C}_{\text{ali}}} + \nu_{\text{C}_{\text{aro}}-\text{C}_{\text{aro}}}$
1436	1521.7	$\nu_{\text{N}=\text{C}}$	1594	1573.5	$\nu_{\text{C}=\text{C}_{\text{cyclopent-3-enyl}}} + \nu_{\text{C}_{\text{ali}}=\text{C}_{\text{ali}}} + \nu_{\text{C}_{\text{aro}}-\text{C}_{\text{aro}}}$
1261	1264.2	$\nu_{\text{C}-\text{N}}$	1504	1520.4	$\nu_{\text{N}-\text{O}}$
1091	1099.3	$\nu_{\text{C}-\text{S}}$	1436	1437.2	$\nu_{\text{C}-\text{N}}$
1012	1044.7	$\nu_{\text{C}_{\text{ali}}-\text{C}_{\text{ali}}}$	1336	1321.6	$\nu_{\text{C}-\text{NO}_2}$
802	821.9	$\omega_{\text{C}_{\text{aro}}-\text{H}}$	1106	1086.5	$\nu_{\text{C}-\text{NO}_2}$
727	772.9	$\nu_{\text{C}-\text{F}}$	975	978.8	$\nu_{\text{C}_{\text{ali}}-\text{C}_{\text{ali}}}$
			852	912.9	$\nu_{\text{C}-\text{C}}$
			759	821.7	$\omega_{\text{C}_{\text{aro}}-\text{H}}$
			721	742.4	$\omega_{\text{C}_{\text{aro}}-\text{H}}$

^[a] ν stretching, α scissoring, ω wagging, δ rocking, ^{aro.}aromatic, ^{ali} aliphatic.

Table 4. ¹H-NMR chemical shifts (δ in ppm) calculated at GIAO/B3LYP/6-31G + (d,p) level in the gas phase.^[a]

Atom	5j Calc.	5k Calc.	5l Calc.	5m Calc.
H1	7.85	7.94	7.97	7.90
H2	8.03	8.11	8.16	8.08
H3	8.77	8.82	8.79	7.77
H4	8.43	8.61	8.60	8.53
H8	4.73	4.60	4.59	4.65
H9	3.35	3.26	3.10	3.17
H9'	4.60	4.63	4.52	4.55
H10	6.98	6.86	6.91	6.86
H11	6.31	6.45	6.40	6.42
H12	4.14	4.29	4.25	4.30
H13	7.23	6.96	7.26	7.05
H14	6.74	6.69	6.54	6.79
H16	7.49	7.45	7.22	7.52
H20	8.19	8.07	7.85	8.18
X1	7.87	7.52	–	7.95
X2	–	–	7.58	–
X3	7.90	7.51	–	7.95

^[a] $\delta = \sum_{\text{X(reference)}} - \sum_{\text{X(reference) (gas)}}$, X = H = 32.27, reference TMS.

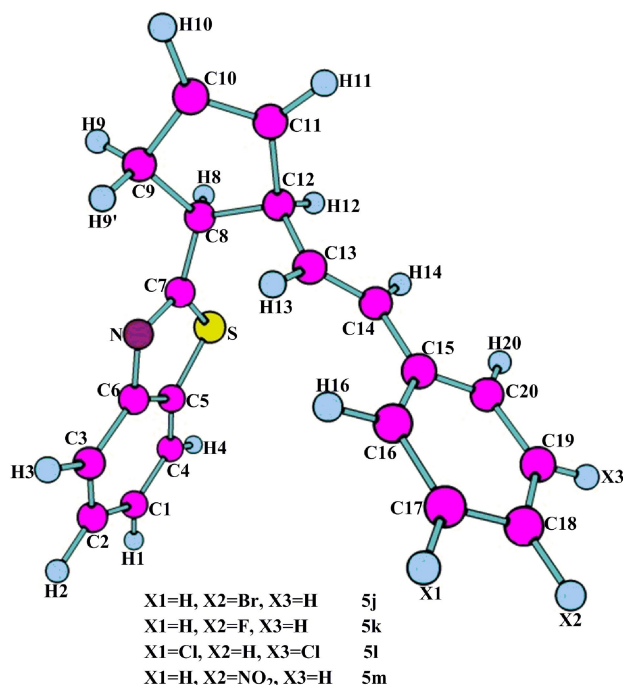


Figure 3. Atom numbering scheme for the molecules of compounds **5j–5m**.

the degeneracy tolerance is 0.1, X3 and H1 give peaks with the same energy and the calculated chemical shift value is 7.90 ppm. This may overlap experimentally with a chemical shift value of 7.43 ppm. X1 in **5j** molecule is hydrogen and the chemical shift value of this hydrogen was calculated to be 7.87 ppm. This calculated chemical shift value may correspond to experimentally 7.38 ppm. The calculated chemical shift value, which corresponds to the chemical shift value of 1H, which is experimentally 7.24 ppm, is 7.49 ppm for H16. The chemical shift value calculated as 7.23 ppm for H13, 6.98 ppm for H10, 6.74 ppm for H14, 6.31 ppm for H11 and 4.60 ppm for H9' may correspond to experimentally 6.43, 6.30, 6.04, 5.78 and 3.77 ppm, respectively. Experimentally, chemical shifts between 3.99–3.88 and 3.16–3.03 ppm were calculated as 4.73 ppm for H8 and 4.14 ppm for H12. The experimental and calculated ¹³C-NMR chemical shift values for the **5j** molecule were compared and the calculated and experimental chemical shift values were found to be very close to each other.

As a result, the chemical shifts of the phenyl ring hydrogen were found as 7–9 ppm, the chemical shifts of the hydrogen atoms attached to the sp³ hybridized carbon were found as 3–4 ppm and an increase was observed in the chemical shift values of hydrogen around the electronegative atoms. All these situations

meet theoretical expectations. As the electron density around a nucleus increase, resonance occurs in the higher field and the NMR signal can be the shift at lower ppm values. The electron donor groups around a nucleus increase electron density around the nucleus and chemical shift value reduces. On the other hand, electron-attracting groups increase the chemical shift value in the nucleus.^[31]

In this section, the calculated chemical shift values are in accordance with experimental values. Similar results were obtained for the molecules of **5k–5m**. The difference between experimental and calculated chemical shift values may be due to the use of different phases in the experiments and in calculation.

Molecular Electrostatic Potential (MEP) Maps

Molecular electrostatic potential (MEP) maps are used to predict the atom with higher electron density in a molecule and this region is called the negative electrostatic region. These regions are open to electrophilic attack and are colored in red shades on standard contour diagrams.^[32] The region of low electron density is the positive electrostatic potential molecule. In this region, the nuclear charge is fully shielded, corresponds to the repulsion of protons and is seen in blue shades on standard contour diagrams.^[33] MEP contour maps denote chemical reactivity, showing nucleophilic and electrophilic sites.^[34] Three-dimensional distribution of MEP is useful to identify the reactive region of a chemical system and to investigate the relationship between molecular structure and physicochemical properties.^[35] With theoretical methods, useful predictions can be made in drug design. It is known that the strong secondary chemical interactions between the produced drug and the target protein are important. MEP maps can be regarded as a reliable identifier of the hydrogen bond.^[36–43] According to the IC₅₀ values of the molecules in *Table 2*, it is the **5c** and **5e** molecules with the greatest biological activity against HeLa and C6 cells, respectively. For this reason, MEP maps of **5c** and **5e** molecules have been investigated. The MEP maps of **5c** and **5e** which calculated B3LYP/6-31G+(d,p) level are given in *Figure 4*.

MEP maps in *Figure 3* indicated that the negative potential regions were localized on the nitrogen atom in the benzothiazole nucleus for **5c** and **5e** molecules. The electron donation of the MeO group in the **5c** molecule is higher than the electron donation of the Me group in the **5e** molecule. This situation may have caused the electron density of the benzothiazole core

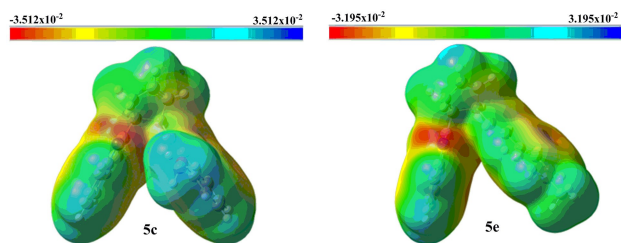


Figure 4. The MEP maps of compounds **5c** and **5e** calculated at B3LYP/6-31G+(d,p) level.

on the **5c** molecule to be higher. The nucleophilic activity increases with the increasing of red zones. In this case, the nucleophilic activity region in the **5c** molecule is more complex. According to MEP maps and electrostatic potential (ESP) derived atomic charges, it is also clear that **5c** will interact more easily with the cancer cells, because the electron density of **5c** is -3.512×10^{-2} and the electron density of **5e** is -3.195×10^{-2} .

Molecular Docking Study

Molecular docking is a computational tool to theoretically examine ligand–protein interactions and is used to obtain binding affinities of a specific receptor ligand.^[44,45] Docking studies were made using free Docking Server program.^[46] The target protein suitable for **5c** and **5e** molecules, which exhibited the highest biological activity against HeLa and C6 cells in docking studies, was obtained from the protein data bank (PDB codes: 1 M17 for HeLa cells and PDB codes: 1JQH for C6 cells) after scanning the articles in the literature.^[47–49]

Molecular docking studies were performed by interacting the **5c** molecule with 1 M17 and the **5e** molecule with 1JQH. In addition, a docking study was conducted to examine the interaction of **5c** and **5e** molecules with 1JQH and 1 M17, respectively. The interaction energies obtained from the molecular docking calculations are given in Table 5. The results in Table 5 show that 1 M17 target protein is suitable for

Table 5. Free binding energies (kcal/mol) of ligands with selected proteins.

Interactions	Free binding energies [kcal mol ⁻¹]
5c molecule with 1JQH	−6.46
5c molecule with 1 M17	−7.78
5e molecule with 1JQH	−8.33
5e molecule with 1 M17	−6.53

5c molecule and 1JQH target protein is suitable for the **5e** molecule.

The interaction energies of **5c** and **5e** molecules with target proteins were calculated to be −7.78 and −8.33 kcal/mol, respectively. The interaction between the ligands and the target protein is shown in Figure 5.

Secondary interactions (the van der Waals (vdW), hydrogen bond and dissolved energy) are considered to predict if a ligand is positioned appropriately to a target protein.^[50] If vdW, hydrogen bond and dissolved energy are negative, the ligand is well attached to an active site on the target molecule. For the **5c** and **5e** molecules, these energy values were −9.30 and −9.24 kcal/mol, respectively. According to the docking server, which gives the binding site analysis, the ligands exhibited a good interaction with the protein in the docking grid.

Drug Likeness Properties

The number of hydrogen bond acceptors (n-ON) and donors (n-OHNN) are within the Lipinski's rules, n-ON < 10 and n-OHNN < 5. The calculated log P must be smaller than 5. In our study, the log P values of **5g** and **5m** were smaller than 5. The molecular weight of the compounds are at the range of 293.38 g/mol and 382.32 g/mol. Compounds **5a**, **5c**, **5e**, **5g** and **5i** can cross blood-brain barrier (BBB). Synthetic accessibility score of the compounds are from 1 (very easy) to 10 (very difficult). Synthetic accessibility of all the compounds are at the range of 3.86 and 4.01. Topological polar surface area (TPSA) must be < 70 Å². TPSA values of all the compounds (except **5m**) were smaller than 70 Å². The solubility (log S) scale value ranges between −10 (insoluble), −6 (poorly soluble), −4 (soluble), −2 (very soluble) and 0 (highly soluble). The solubility of compounds was poorly soluble. The more negative the skin permeation (log Kp) the less skin permeant the molecule. For example, Diclofenac is a good topic anti-inflammatory with a predicted log Kp = −4.96 (cm/s), while Ouabain has little chance to cross skin with a predicted log Kp = −10.94 (cm/s). The log Kp of the compounds −3.62 and −4.67 cm/s.

According to Lipinski's rule of five; the compounds could be a new potential anticancer agent according to calculated data (Table 6).^[51]

The pink area represents the optimal range for each properties (lipophilicity: LOGP between −0.7 and +5.0, size: MW between 150 and 500 g/mol, polarity: TPSA between 20 and 130 Å², solubility: log S not higher than 6, saturation: fraction of carbons in the sp³ hybridization not less than 0.25, and flexibility: no

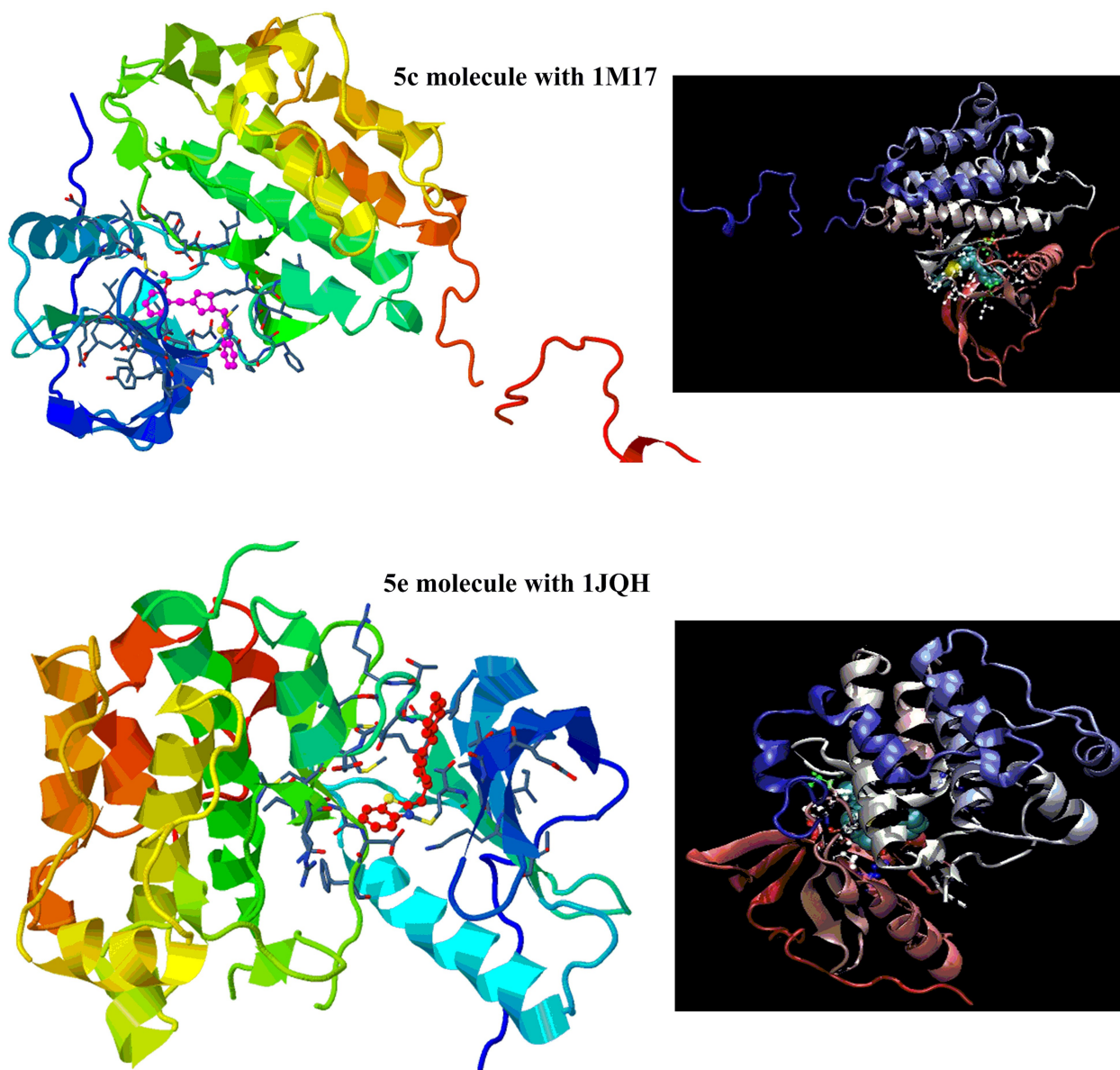


Figure 5. Interaction of molecule **5c** (pink balls) with protein 1M17 and that of molecule **5e** (red balls) with protein 1JQH.

more than 9 rotatable bonds). In this example, the compound is predicted not orally bioavailable, because of being too flexible and too polar. Bioavailability radar of **5e** is demonstrated in Figure 6.

Conclusions

In this study, antiproliferative activity of the compounds **5a–5m** was tested against C6 and HeLa cell lines. According to the results, **5a–5m** have significant antiproliferative activity compared with 5-fluorouracil and cisplatin against both HeLa and C6 cell lines. The

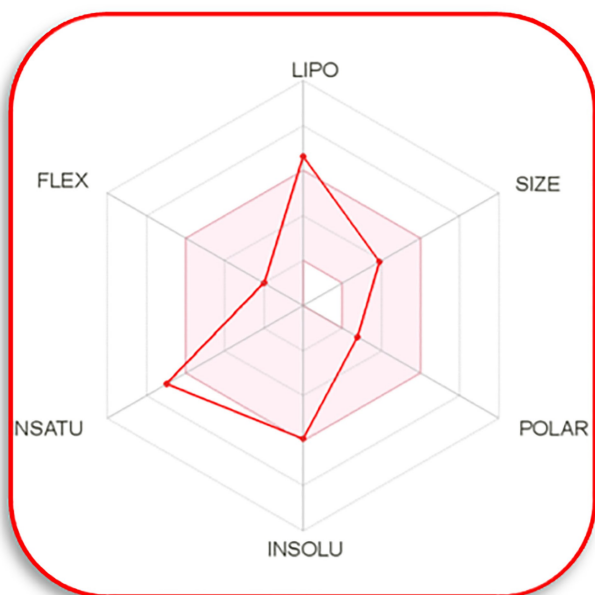
most active compound was **5e** against C6 cell lines with $IC_{50} = 5.89 \mu\text{M}$ (cisplatin, $IC_{50} = 14.46 \mu\text{M}$ and 5-FU, $IC_{50} = 76.74 \mu\text{M}$). Furthermore, the most active compounds were **5c** and **5g** against HeLa cell lines with $IC_{50} = 3.98 \mu\text{M}$ and $6.19 \mu\text{M}$ (cisplatin, $IC_{50} = 37.95 \mu\text{M}$ and 5-FU, $IC_{50} = 46.32 \mu\text{M}$). These compounds appear to be promising anticancer agents, especially against these cell lines.

Additionally, computational studies of **5a–5m** are performed by using B3LYP/6-31G+(d,p) level. Afterwards, experimental and calculated IR and NMR results are compared with each other. Due to the harmony between experimental and calculated frequencies in

Table 6. Drug-likeness properties of the compounds.^[a]

No.	Log P	TPSA [Å ²]	MW [g/mol]	nON	nOHNH	Log S	Lipinski [Pfizer]	Synthetic accessibility	BBB	log Kp [cm/s]
5a	5.03	50.36	333.45	2	0	-5.69	0.55	3.92	yes	-4.29
5b	5.61	41.13	337.87	1	0	-6.22	0.55	3.86	no	-3.85
5c	5.03	50.36	333.45	4	2	-5.69	0.55	3.99	yes	-4.29
5d	5.69	41.13	382.32	3	1	-6.53	0.55	3.91	no	-4.08
5e	5.40	41.13	317.45	3	1	-5.92	0.55	3.99	yes	-3.92
5f	5.04	69.37	309.45	1	0	-5.47	0.55	3.94	no	-4.33
5g	4.38	54.27	293.38	2	0	-4.99	0.55	3.92	yes	-4.67
5h	5.69	41.13	382.32	1	0	-6.53	0.55	3.91	no	-4.08
5i	5.40	41.13	317.45	3	1	-5.92	0.55	4.01	yes	-3.92
5j	5.69	41.13	382.32	1	0	-6.53	0.55	3.88	no	-4.08
5k	5.38	41.13	321.41	2	0	-5.78	0.55	3.85	no	-4.13
5l	6.05	41.13	372.31	1	0	-6.80	0.55	3.95	no	-3.62
5m	4.46	86.95	348.42	3	0	-5.68	0.55	3.97	no	-4.48

^[a] These parameters were determined with Swiss ADME predictor.

**Figure 6.** The bioavailability radar of compound **5e**.

the vibrational spectra of molecules, accurate predictions can be made with computational chemistry methods in this study. The active regions of **5c** and **5e** are determined by MEP map. Moreover, according to the electrostatic potential (ESP) atomic loads derived from MEP maps, **5c** has been found to interact more easily with the cancer cell lines, because the electron density of **5c** is -3.512×10^{-2} and the electron density of **5e** is -3.195×10^{-2} . Additionally, chemical reactivity of **5a–5m** is determined by using molecular docking. The interaction energies of **5c** and **5e** molecules with target proteins were calculated as -7.78 and

-8.33 kcal/mol, respectively. As a result, selected target proteins are highly suitable for molecules. These molecules can be applied to the related cancer cell lines.

According to Lipinski's rule of five, compounds **5a–5m** could be new potential anticancer agents according to calculated data. However, **5e** was the most effective compounds against C6 cell lines ($IC_{50} = 5.89 \mu\text{M}$) and can pass BBB.

Experimental Section

General

All reagents and solvents were purchased from Sigma-Aldrich and Merck and were used without further purification. Dulbecco's modified eagle's medium (DMEM), fetal bovine serum and PenStrep solution, 5-fluorouracil, cisplatin were purchased from Sigma Chemicals (Germany). 96-Well culture plates were obtained from COSTAR, Corning (USA). BrdU Cell Proliferation ELISA assay reagent was purchased from Roche (Germany). The purity of the synthesized compounds is above 98% according to the results of the elemental analysis. UV spectra were recorded on JASCO V 530. NMR spectra were recorded on a Bruker Avance III 400 spectrometer in CDCl_3 . Chemical shifts are reported in parts per million (δ) and were referenced to the residual solvent signal (CDCl_3 : 7.28 and 77.00 ppm for ^1H and ^{13}C , respectively). Melting points (m.p.) were measured with an Electrothermal 9100 apparatus and uncorrected. IR spectra (KBr disc) were measured on a Jasco FT/IR-430 spectrometer.

The elemental analyses were obtained from a Leco CHNS 9932 elemental analyzer.

Synthesis of 7-Benzylidenebicyclo[3.2.0]hept-2-en-6-ones **3a–3m**

The starting compounds **3a–3m** were synthesized by our previously published procedure.^[23]

(1R,5S,7E)-7-[(4-Bromophenyl)methylidene]bicyclo[3.2.0]hept-2-en-6-one (3j). Yield 97%. M.p. 95–97 °C (AcOEt/hexane (1:9)). White solid. IR (KCl, cm^{-1}): 3444, 3057, 301, 2918, 2899, 1736, 1636, 1484, 1399, 1154, 1069, 906, 811, 717, 533, 472. $^1\text{H-NMR}$ (400 MHz, CDCl_3): 7.52 (d, $J=8.4$, 2H), 7.42 (d, $J=8.4$, 2H), 6.77 (s, 1H), 5.98–5.96 (m, 1H), 5.87–5.86 (m, 1H), 4.35–4.34 (m, 1H), 4.02–3.9 (m, 1H); 2.84 (bd, $J=17.6$, 1H), 2.64 (dd, $J=17.6$, 12.0, 1H). $^{13}\text{C-NMR}$ (100 MHz, CDCl_3): 203.6, 149.9, 133.6, 133.1, 132.2 (2 C), 131.1 (2 C), 128.3, 124.3, 122.8, 60.8, 49.6, 34.7. Anal. calc. for $\text{C}_{14}\text{H}_{11}\text{BrO}$: C, 61.11; H, 4.03; Found: C, 61.13; H, 4.06.

(1R,5S,7E)-7-[(4-Fluorophenyl)methylidene]bicyclo[3.2.0]hept-2-en-6-one (3k). The title compound was prepared in a yield of 98%. M.p. 81–82 °C (AcOEt/hexane (1:9)). White solid. IR (KCl, cm^{-1}): 2954; 2867; 2852; 1731; 1643; 1598; 1508; 1224; 1149; 1085; 1043; 921; 831; 809. $^1\text{H-NMR}$ (400 MHz, CDCl_3): 7.59 (dd, $J=8.8$, 5.6, 2H), 7.12 (t, $J=8.8$, 2H), 6.84 (d, $J=2.0$, 1H), 6.03–6.00 (m, 1H), 5.90–5.88 (m, 1H), 4.38–4.37 (m, 1H), 3.95–3.92 (m, 1H), 2.83–2.77 (d, $J=15.2$, 1H), 2.64–2.56 (ddd, $J=15.2$, 8.8, 2.9, 1H). $^{13}\text{C-NMR}$ (100 MHz, CDCl_3): 203.7, 164.8, 162.3, 148.9, 133.6, 131.8, 131.7, 130.5, 130.4, 128.5, 123.0, 116.4, 116.1, 60.7, 49.4, 34.7. Anal. calc. for $\text{C}_{14}\text{H}_{11}\text{FO}$: C, 78.49; H, 5.18; Found: C, 78.44; H, 5.15.

(1R,5S,7E)-7-[(2,5-Dichlorophenyl)methylidene]bicyclo[3.2.0]hept-2-en-6-one (3l). The title compound was prepared in a yield of 87%. M.p. 16–169–97 °C (AcOEt/hexane (1:9)). White solid. IR (KCl, cm^{-1}): 3068; 2950; 2861; 1747; 1641; 1558; 1417; 1245; 1147; 1085; 1043; 937; 852; 802. $^1\text{H-NMR}$ (400 MHz, CDCl_3): 7.43 (m, 2H), 7.38 (m, 1H), 6.72 (s, 1H), 6.01–5.98 (m, 2H), 5.94–5.92 (m, 1H), 4.43–4.41 (m, 1H), 3.99–3.94 (m, 1H), 2.85–2.79 (bd, $J=17.6$, 1H), 2.66–2.58 (dd, $J=17.6$, 10.2, 1H). $^{13}\text{C-NMR}$ (100 MHz, CDCl_3): 203.3, 151.7, 137.2, 1335.6, 134.1, 129.5, 127.9, 127.7, 121.1, 61.2, 49.7, 34.9. Anal. calc. for $\text{C}_{14}\text{H}_{10}\text{Cl}_2\text{O}$: C, 63.42; H, 3.80; Found: C, 63.39; H, 3.83.

(1R,5S,7E)-7-[(4-Nitrophenyl)methylidene]bicyclo[3.2.0]hept-2-en-6-one (3m). The title compound was prepared in a yield of 81%. M.p. 99–101 °C (AcOEt/hexane (1:9)). White solid. IR (KCl, cm^{-1}): 2958; 2933; 2861; 2358; 1745; 1637; 1592; 1508; 1344; 1149; 1087; 904; 848. $^1\text{H-NMR}$ (400 MHz, CDCl_3): 8.28 (d, $J=8.8$, 2H), 7.74 (d, $J=8.8$, 2H), 6.89 (s, 1H), 6.00–5.94 (m, 2H), 4.48–4.46 (m, 1H), 3.92–3.88 (m, 1H); 2.78 (bd, $J=17.6$, 1H), 2.58 (dd, $J=17.6$, 10.4, 1H). $^{13}\text{C-NMR}$ (100 MHz, CDCl_3): 203.3, 153.1, 147.9, 140.6, 134.4, 130.2 (2 C), 127.7, 124.2 (2 C), 121.2, 61.3, 49.9, 35.1. Anal. calc. for $\text{C}_{14}\text{H}_{11}\text{NO}_3$: C, 69.70; H, 4.60; N, 5.81; Found: C, 69.68; H, 4.62; N, 5.84.

Synthesis of 2-[2-(2-Phenylethenyl)cyclopent-3-en-1-yl]-1,3-benzothiazoles **5a–5m**

The compounds **5a–5m** were synthesized by our previously published procedure.^[24]

2-[(1S,2S)-2-[(E)-2-(4-Bromophenyl)ethenyl]cyclopent-3-en-1-yl]-1,3-benzothiazole (5j). The title compound was prepared in a yield of 98%. Viscous oil. IR (KBr, cm^{-1}): 3056 (m), 2929 (s), 2850 (m), 1590 (m), 1436 (s), 1311 (m), 1241 (m), 1108 (m), 964 (m), 759 (m), 728 (s), 682 (m). $^1\text{H-NMR}$ (400 MHz, CDCl_3): 8.01 (d, $J=8.1$, 1H), 7.87 (d, $J=8.0$, 1H), 7.48 (t, $J=7.5$, 1H), 7.43 (d, $J=8.3$, 2H), 7.38 (t, $J=7.5$, 1H), 7.24 (d, $J=8.3$, 2H), 6.43 (d, $J=15.8$, 1H), 6.30 (dd, $J=15.8$, 7.9, 1H), 6.04–5.88 (m, 2H), 5.78 (dd, $J=5.7$, 2.3, 1H), 3.99–3.88 (m, 1H), 3.77 (q, $J=7.7$, 1H), 3.16–3.03 (m, 1H), 3.00–2.89 (m, 1H). $^{13}\text{C-NMR}$ (101 MHz, CDCl_3): 174.6, 153.1, 146.4, 143.3, 135.8, 134.2, 131.3, 130.7, 128.4, 126.5, 126.3, 124.7, 123.9, 122.5, 121.3, 56.6, 50.1, 40.2. Anal. calc. for $\text{C}_{20}\text{H}_{16}\text{BrNS}$: C, 62.83; H, 4.22; N, 3.66; S, 8.39; Found: C, 62.81; H, 4.21; N, 3.67; S, 8.37.

2-[(1S,2S)-2-[(E)-2-(4-Fluorophenyl)ethenyl]cyclopent-3-en-1-yl]-1,3-benzothiazole (5k). The title compound was prepared in a yield of 92%. Viscous oil. IR (KBr, cm^{-1}): 3056 (w), 2962 (s), 2850 (m), 1646 (m), 1509 (s), 1436 (m), 1261 (s), 1012 (m), 802 (m), 727 (s). $^1\text{H-NMR}$ (400 MHz, CDCl_3): 8.02 (d, $J=8.2$, 1H), 7.87 (d, $J=7.8$, 1H), 7.48 (ddd, $J=8.3$, 7.2, 1.3, 2H), 7.43–7.31 (m, 4H), 7.06–6.97 (m, 2H), 6.46 (d, $J=15.8$, 1H), 6.22 (dd, $J=15.8$, 8.0, 1H), 5.98–5.92 (m, 1H), 5.82–5.76 (m, 1H), 3.99–3.87 (m, 1H), 3.77 (dt, $J=8.8$, 7.3, 1H), 3.16–3.03 (m, 1H), 3.00–2.89 (m, 1H). $^{13}\text{C-NMR}$ (101 MHz, CDCl_3): 174.8, 153.1, 134.9, 132.4, 131.2, 131.2, 130.2, 129.6, 127.8, 127.7, 125.9, 124.8, 122.7, 121.5, 115.5, 115.3, 56.6, 50.3, 40.1. Anal. calc. for $\text{C}_{20}\text{H}_{16}\text{FNS}$: C,

74.74; H, 5.02; N, 4.36; S, 9.98; Found: C, 74.71; H, 5.00; N, 4.38; S, 9.94.

2-((1S,2S)-2-[(E)-2-(2,5-Dichlorophenyl)ethenyl]cyclopent-3-en-1-yl)-1,3-benzothiazole (5l). The title compound was prepared in a yield of 94%. Viscous oil. IR (KBr, cm^{-1}): 3056 (w), 2962 (s), 2850 (m), 1646 (m), 1509 (s), 1436 (m), 1261 (s), 1091 (w), 982 (m), 802 (m), 727 (s). $^1\text{H-NMR}$ (400 MHz, CDCl_3): 8.02 (d, $J=8.1$, 1H), 7.87 (d, $J=8.0$, 1H), 7.49 (td, $J=7.6$, 3.2, 2H), 7.39 (td, $J=7.3$, 1H), 7.27–7.18 (m, 3H), 6.36 (d, $J=6.2$, 2H), 5.99–5.93 (m, 1H), 5.79–5.73 (m, 1H), 3.94 (q, $J=3.3$, 2.8, 1H), 3.76 (q, $J=7.8$, 1H), 3.15–3.04 (m, 1H), 3.00–2.90 (m, 1H), 1.69 (s, 1H). $^{13}\text{C-NMR}$ (101 MHz, CDCl_3): 174.4, 140.1, 135.1, 134.5, 132.2, 130.7, 128.4, 127.1, 126.0, 124.8, 124.6, 122.7, 121.6, 56.5, 50.1, 40.1. Anal. calc. for $\text{C}_{20}\text{H}_{15}\text{Cl}_2\text{NS}$: C, 64.52; H, 4.06; N, 3.76; S, 8.61; Found: C, 64.50; H, 4.08; N, 3.78; S, 8.63

2-((1S,2S)-2-[(E)-2-(4-Nitrophenyl)ethenyl]cyclopent-3-en-1-yl)-1,3-benzothiazole (5m). The title compound was prepared in a yield of 91%. Viscous oil. IR (KBr, cm^{-1}): 3064 (m), 2971 (s), 2940 (m), 1635 (w), 1594 (w), 1504 (m), 1436 (w), 1336 (m), 1106 (w), 975 (w), 852 (w), 759 (w), 721 (w). $^1\text{H-NMR}$ (400 MHz, CDCl_3): 8.18 (d, $J=8.1$, 2H), 8.01 (d, $J=8.1$, 1H), 7.88 (d, $J=8.0$, 1H), 7.61–7.44 (m, 3H), 7.39 (t, $J=7.6$, 1H), 6.64–6.47 (m, 2H), 6.06–5.95 (m, 1H), 5.85–5.76 (m, 1H), 4.01 (ddt, $J=6.9$, 4.5, 2.2, 1H), 3.80 (dt, $J=8.8$, 7.4, 1H), 3.12 (ddt, $J=13.3$, 6.7, 2.2, 1H), 3.02–2.89 (m, 1H). $^{13}\text{C-NMR}$ (100 MHz, CDCl_3): 174.3, 153.0, 146.7, 143.6, 136.6, 134.8, 131.6, 130.9, 128.8, 126.8, 126.1, 124.9, 123.9, 122.7, 121.5, 56.6, 50.1, 40.2. Anal. calc. for $\text{C}_{20}\text{H}_{16}\text{N}_2\text{O}_2\text{S}$: C, 68.94; H, 4.63; N, 8.04; S, 9.20; Found: C, 68.90; H, 4.60; N, 8.07; S, 9.22.

Preparation of Standards and Samples Solution

Stock solutions of compounds **5a–5m**, 5-fluorouracil and cisplatin were dissolved in sterile DMSO and diluted Dulbecco's modified Eagle's medium (DMEM; 1:20). DMSO final concentration is below 1% in all tests.

Cell Culture and Cell Proliferation Assay

HeLa (human cervix carcinoma) and C6 (rat brain tumor) cells were grown in Dulbecco's modified Eagle's medium, supplemented with 10% (v/v) fetal bovine serum and 2% (v/v) PenStrep solution at 37 °C in a 5% CO_2 humidified atmosphere. Firstly, cells were plated in 96-well culture plates at a density of 30,000

cells per well. 5-Fluorouracil, cisplatin and several of the samples in various concentrations (100–500 μM) were added to each well. Cells were incubated overnight. Afterward, the BrdU Cell Proliferation ELISA assay reagent was applied according to the manufacturer's procedure. The amount of cell proliferation was assessed by determining the absorbance at 450 nm by using a micro-plate reader (Ryto, China). Results were reported as IC_{50} values (Table 2).

Determination of IC_{50} Values

Determination of IC_{50} values: The half-maximal inhibitory concentration (IC_{50}) is a measure of the effectiveness of a compound in inhibiting biological function. In this article, IC_{50} values was determined using ED50 plus v1.0.

Computational Method

The investigated compounds were drawn with the Gauss View 5.0.8 package program for molecular geometry optimization^[52] and the calculation was performed via Gaussian 09 Revision D.01 program pack (Linux based) in TUBITAK-TR Grid.^[53] The calculations included Density Functional Theory (DFT) hybrid B3LYP^[54] and used 6–31G+(d,p) basic sets. Molecular geometries were optimized using B3LYP/6–31G+(d,p) level in the gas phase. IR spectra obtained as harmonic were converted to inharmonic frequencies with a scale factor of 0.9640.^[28] The ^1H - and ^{13}C -NMR chemical shift were calculated with the gauge-including atomic orbital (GIAO) approach by using B3LYP/6–31G+(d,p) level of the compounds **5j–5m**.

The B3LYP/6–31G+(d,p) level, which is preferred in the computational studies of organic molecules in recent years, is in the large basic set group.^[55–57] Large basic sets adjust the orbitals correctly, with fewer restrictions on the location of electrons in space. The basic set of B3LYP/6–31G+(d,p), which adds p functions to hydrogen atoms in addition to the d functions on heavy atoms, analyses the space locations of electrons in a large region.^[58]

Physicochemical and Pharmacokinetic Properties for Computational Methods

Programming and Scripting. The SwissADME website was written in HTML, PHP5, and JavaScript, whereas the backend of computation was mainly coded in Python 2.7. The use of additional libraries or software

for specific tasks is mentioned in the corresponding paragraph.

Submission Page. The molecule input through the sketcher Marvin JS (version 16.4.18, 2016, www.chemaxon.com) are converted into SMILES by JChem Web Services (version 14.9.29, 2013, www.chemaxon.com) installed on one of our servers. This on-the-fly conversion allows seamless paste of SMILES in the input list. The user has the possibility to edit this list as a standard text, e.g., to modify SMILES or add a name to the molecule. www.nature.com/scientificreports/SCientificREpOrtS/7:42717/ DOI: 10.1038/srep42717 9 Upon calculation submission by clicking the 'Run' button, the SMILES of each molecule is canonicalized by OpenBabel (version 2.3.0, 2012, http://openbabel.org) 9 and processed individually.^[51]

Acknowledgements

The authors are indebted to the Department of Chemistry at Gaziosmanpasa University and TUBITAK (Scientific and Technological Council of Turkey) (Project No. 111T111) for their support. The numerical calculations reported in this article are performed at TUBITAK ULAKBIM, High Performance and Grid Computing Center (TRUBA Resources).

Author Contribution Statement

M. C., N. A., and E. K. designed and performed the experiments, analyzed the data. M. C. wrote the article. A. S. Y. performed the anticancer activity experiments, analyzed the data and determined the drug likeness properties of compounds. S. E. carried out molecular docking study and MEP maps of compounds.

References

- [1] M. N. Noolvi, H. M. Patel, M. Kaur, 'Benzothiazoles: Search for anticancer agents', *Eur. J. Med. Chem.* **2012**, *54*, 447–462.
- [2] W. Liu, X. Zhang, J. Zhao, J. Li, Z. Cui, X. Mao, 'Inhibition of cervical cancer cell metastasis by benzothiazole through up-regulation of E-cadherin expression', *Microb. Pathog.* **2017**, *111*, 182–186.
- [3] G. Turan-Zitouni, Y. Ozkay, A. Ozdemir, Z. A. Kaplancikli, M. D. Altintop, 'Synthesis of Some Benzothiazole Based Piperazine-Dithiocarbamate Derivatives and Evaluation of Their Anticancer Activities', *Lett. Drug Des. Discovery* **2011**, *8*, 830–837.
- [4] S. H. L. Kok, R. Gambari, H. C. Chung, O. T. C. Johny, C. Filly, S. C. C. Albert, 'Synthesis and anti-cancer activity of benzothiazole containing phthalimide on human carcinoma cell lines', *Bioorg. Med. Chem.* **2008**, *16*, 3626–3631.
- [5] M. Wang, M. Gao, B. H. Mock, K. Miller, G. W. Sledge, G. D. Hutchins, Q. Zheng, 'Synthesis of carbon-11 labeled fluorinated 2-arylbenzothiazoles as novel potential PET cancer imaging agents', *Bioorg. Med. Chem.* **2006**, *14*, 8599–8607.
- [6] C. G. Mortimer, G. Wells, J. P. Crochard, E. L. Stone, T. D. Bradshaw, M. F. G. Stevens, A. D. Westwell, 'Antitumor Benzothiazoles. 26. (1)2-(3,4-Dimethoxyphenyl)-5-fluoroben-zothiazole (GW 610, NSC 721648), a Simple Fluorinated 2-Arylbenzothiazole, Shows Potent and Selective Inhibitory Activity against Lung, Colon, and Breast Cancer Cell Lines', *J. Med. Chem.* **2006**, *49*, 179–185.
- [7] A. Irfan, F. Batool, S. A. Z. Naqvi, A. Islam, S. M. Osman, A. Nocentini, S. A. Alissa, C. T. Supuran, 'Benzothiazole derivatives as anticancer agents', *J. Enzyme Inhib. Med. Chem.* **2015**, *35*, 265–279.
- [8] F. Piscitelli, C. Ballatore, A. Smith, 'Solid phase synthesis of 2-aminobenzothiazoles', *Bioorg. Med. Chem.* **2010**, *20*, 644–648.
- [9] D.-Q. Li, X.-L. Deng, H.-Y. Zhao, F.-C. Zhang, R.-E. Liu, 'Inhibition of tumor growth and angiogenesis by 2-(4-aminophenyl) benzothiazole in ortho topic glioma C6 rat model', *Saudi J. Biol. Sci.* **2018**, *25*, 1483–1487.
- [10] M. N. Noolvi, H. M. Patel, M. Kaur, 'Benzothiazoles: search for anticancer agents', *Eur. J. Med. Chem.* **2012**, *54*, 447–462.
- [11] M. Yoshida, I. Hayakawa, I. Hayashi, T. Agatsuma, Y. Oda, F. Tanzawa, S. Iwasaki, K. Koyama, H. Furukawa, S. Kurakata, Y. Sugano, 'Synthesis and biological evaluation of benzothiazole derivatives as potent antitumor agents', *Bioorg. Med. Chem.* **2005**, *15*, 3328–3332.
- [12] L. Racan, M. Kralj, L. Suman, R. Stojkovic, V. Tralic-Kulenovic, G. Karminski-Zamola, 'Novel amidino substituted 2-phenylbenzothiazoles: Synthesis, antitumor evaluation *in vitro* and acute toxicity testing *in vivo*', *Bioorg. Med. Chem.* **2010**, *18*, 1038–1044.
- [13] M. M. Uremis, A. Sahin Yaglioglu, Y. Budak, M. Ceylan, 'Synthesis, characterization, *in vitro* antiproliferative and cytotoxicity effects of a new class of 2-((1R,2S)-2-((E)-4-substitutedstyryl)cyclooctyl)benzo[d]thiazole derivatives', *Org. Commun.* **2017**, *10*, 190–200.
- [14] N. Uremis, M. M. Uremis, I. F. Tolun, M. Ceylan, A. Doganer, A. Kurt, 'Synthesis of 2-substituted benzothiazole derivatives and their *in vitro* anticancer effects and antioxidant activities against pancreatic cancer cells', *Anticancer Res.* **2017**, *37*, 6381–6389.
- [15] H. A. Bhuvu, S. G. Kini, 'Synthesis, anticancer activity and docking of some substituted benzothiazoles as tyrosine kinase inhibitors', *J. Mol. Graph. Model.* **2010**, *9*, 32–37.
- [16] M. N. Noolvi, H. M. Patel, M. Kaur, 'Benzothiazoles: search for anticancer agents', *J. Med. Chem.* **2012**, *54*, 447–462.
- [17] V. R. Solomon, C. Hua, H. Lee, 'Hybrid pharmacophore design and synthesis of isatin-benzo-thiazole analogs for their anti-breast cancer activity', *Bioorg. Med. Chem.* **2009**, *17*, 7585–7592.
- [18] G. Wells, T. D. Bradshaw, P. Diana, A. Seaton, D. F. Shi, A. D. Wetwell, M. F. G. Stevens, 'Anti-tumor benzothiazoles.

- Part 10: the synthesis and anti-tumor activity of benzothiazole substituted quinol derivatives', *Bioorg. Med. Chem. Lett.* **2000**, *10*, 513–515.
- [19] D. T. K. Oanh, H. V. Hai, S. H. Park, H. J. Kim, B. W. Han, H. S. Kim, J. T. Hong, S. B. Han, V. T. Hue, N. H. Nama, 'Benzothiazole-containing hydroxamic acids as histone deacetylase inhibitors and antitumor agents', *Bioorg. Med. Chem. Lett.* **2011**, *21*, 7509–7512.
- [20] D. S. Prasanna, C. V. Kavitha, K. Vinaya, S. R. Ranganatha, S. C. Raghavan, K. S. Rangappa, 'Synthesis and Identification of a new class of antileukemic agents containing 2-(arylcarboxamide)-(S)-6-amino-4,5,6,7-tetrahydrobenzo[d]thiazole', *Eur. J. Med. Chem.* **2010**, *45*, 5331–5336.
- [21] M. Bavadi, K. Nikman, O. Shahraki, 'Novel pyrrole derivatives bearing sulfonamide groups: Synthesis *in vitro* cytotoxicity evaluation, molecular docking and DFT study', *J. Mol. Struct.* **2017**, *1146*, 242–253.
- [22] S. Lakshmanan, D. Govindaraj, N. Ramalakshmi, S. Arul Antony, 'Synthesis, molecular docking, DFT calculations and cytotoxicity activity of benzo[g]quinazoline derivatives in choline chloride-urea', *J. Mol. Struct.* **2017**, *1150*, 88–95.
- [23] M. Ceylan, E. Findik, 'Synthesis and characterization of new chalcone derivatives from *cis*-bicyclo[3.2.0]hept-2-en-6-one', *Synth. Commun.* **2009**, *39*, 1046–1054.
- [24] E. Findik, 'Synthesis of the novel benzothiazole compounds from 7-benzylidenebicyclo[3.2.0]hept-2-en-6-ones and 2-aminobenzenethiol', *Turk. J. Chem.* **2012**, *36*, 93–100.
- [25] G. Ceyhan, M. Kose, M. Tumer, I. Demirtas, A. Sahin Yaglioglu, V. McKee, G. Ceyhan, M. Kose, M. Tumer, I. Demirtas, A. S. Yaglioglu, V. McKee, 'Structural characterization of some Schiff base compounds: Investigation of their electrochemical, photoluminescence, thermal and anticancer activity properties', *J. Lumin.* **2013**, *143*, 623–634.
- [26] G. Karakuş, Z. A. Polat, A. S. Yaglioglu, M. Karahan, A. F. Yenidünya, 'Synthesis, characterization, and assessment of cytotoxic, antiproliferative, and antiangiogenic effects of a novel procainamide hydrochloride-poly (maleic anhydride-co-styrene) conjugate', *J. Biomater. Sci. Polym. Ed.* **2013**, *10*, 1260–1276.
- [27] P. J. Stephens, F. J. Devlin, C. F. Chabalowski, M. J. Frisch, 'Ab initio calculation of vibrational absorption and circular dichroism spectra using density functional force fields', *J. Phys. Chem. C* **1994**, *98*, 11623–11627.
- [28] <http://cccbdb.nist.gov/vibscalejustx.asp>.
- [29] M. Mirzaei, '5-Fluorouracil: Computational Studies of Tautomers and NMR Properties', *Turk. Comput. Theor. Chem.* **2017**, *1*, 27–34.
- [30] F. Purtaş, K. Sayin, G. Ceyhan, M. Köse, M. Kurtoglu, 'New fluorescent azo-Schiff base Cu(II) and Zn(II) metal chelates; spectral, structural, electrochemical, photoluminescence and computational studies', *J. Mol. Struct.* **2017**, *137*, 461–475.
- [31] K. Sayin, D. Karakas, 'Structural, spectral, NLO and MEP analysis of the [MgO₂Ti₂(OPri)₆], [MgO₂Ti₂(OPri)₂(acac)₄] and [MgO₂Ti₂(OPri)₂(bzac)₄] by DFT method', *Spectrochim. Acta A* **2015**, *144*, 176–182.
- [32] G. C. Muscia, S. I. Cazorla, F. M. Frank, G. L. Borosky, G. Y. Buldain, S. E. Asis, E. L. Malchiodi, 'Synthesis, trypanocidal activity and molecular modeling studies of 2-alkylaminomethylquinoline derivatives', *J. Med. Chem.* **2011**, *46*, 3696–3703.
- [33] P. S. Kushwaha, P. C. Mishra, 'Relationship of hydrogen bonding energy with electrostatic and polarization energies and molecular electrostatic potentials for amino acids: an evaluation of the lock and key model', *Int. J. Quant. Chem.* **2000**, *76*, 700–713.
- [34] M. Wagener, J. Sadowysky, J. Gasteiger, 'Autocorrelation of molecular surface properties for modeling corticosteroid binding globulin and cytosolic Ah receptor activity by neural networks', *J. Am. Chem. Soc.* **1995**, *117*, 7769–7775.
- [35] J. Jayabharathi, V. Thanikachalam, M. Venkatesh Perumal, N. Srinivasan, 'Fluorescence resonance energy transfer from a bio-active imidazole derivative 2-(1-phenyl-1H-imidazo[4,5-f][1,10]phenanthroline-2-yl)phenol to a bioactive indoloquinolizine system', *Spectrochim. Acta A* **2011**, *79*, 236–244.
- [36] A. Kumar, C. G. Mohan, P. C. Mishra, 'Molecular electrostatic potential and field as descriptors of hydrogen bonding and molecular activity. Effects of hybridization displacement charge', *J. Mol. Struct.-Theochem.* **1996**, *361*, 135–144.
- [37] C. Santosh, P. C. Mishra, 'Structure-activity relationship for some 2,3-dideoxynucleoside anti-HIV drugs using molecular electrostatic potential mapping', *J. Mol. Model.* **1997**, *3*, 172–181.
- [38] P. C. Mishra, A. Kumar, J. S. Muray, K. D. Sen, 'Theoretical and Computational Chemistry Book Series', Amsterdam, Elsevier, 1996.
- [39] A. K. Singh, P. S. Kushwaha, P. C. Mishra, 'Near ab initio quality molecular electrostatic potential maps using hybridization displacement charges at PM3 level and effects of geometrical changes in amino groups', *Int. J. Quant. Chem.* **2001**, *82*, 299–312.
- [40] M. K. Shukla, P. C. Mishra, 'Structure-activity relationship for some xanthenes as adenosine A1 receptor antagonists, bronchodilators and phosphodiesterase inhibitors: an electric field mapping approach', *J. Mol. Struct.-Theochem.* **1995**, *340*, 159–167.
- [41] B. Tüzün, 'Theoretical Evaluation of Six Indazole Derivatives as Corrosion Inhibitors Based on DFT', *Turk. Comput. Theor. Chem.* **2018**, *2*, 12–22.
- [42] M. Kose, C. Hepokur, D. Karakuş, V. McKee, M. Kurtoglu, 'Structural, computational and cytotoxic studies of square planar copper(II) complexes derived from dicyandiamide', *Polyhedron* **2016**, *117*, 652–660.
- [43] M. S. Almutari, A. M. Alanazi, E. S. Al-Abdullah, A. A. El-Emam, S. K. Pathak, R. Srivastava, O. Prasad, L. Sinha, 'FT-IR and FT-Raman spectroscopic signatures, vibrational assignments, NBO, NLO analysis and molecular docking study of 2-[[5-(adamantan-1-yl)-4-methyl-4H-1,2,4-triazol-3-yl]sulfanyl]-N,N-dimethylethanamine', *Spectrochim. Acta A* **2015**, *140*, 1–14.
- [44] A. K. Singh, R. K. Singh, 'DFT and molecular docking studies on 2-(2-mercaptophenylimino)-4-methyl-2H-chromen-7-ol', *J. Mol. Struct.* **2016**, *1122*, 318–323.
- [45] Z. Bikadi, E. Hazai, Z. Bikadi, E. Hazai, 'Application of the PM6 semi-empirical method to modeling proteins enhances docking accuracy of AutoDock', *J. Cheminform.* **2009**, *15*, 1–16.
- [46] B. Misselwitz, S. K. Kreibich, S. Rout, B. Stecher, B. Periaswamy, W. D. Hardt, 'Salmonella enterica serovar Typhimurium binds to HeLa cells via Fim-mediated rever-

- sible adhesion and irreversible type three secretion system 1-mediated docking', *Infect. Immun.* **2011**, *709*, 340–341.
- [47] A. S. El-Azab, M. A. Al-Omar, A. A. M. Abdel-Aziz, N. I. Abdel-Aziz, M. A. A. El-Sayed, A. M. Aleisa, M. M. Sayed-Ahmed, S. G. Abdel-Hamide, 'Design, synthesis and biological evaluation of novel quinazoline derivatives as potential antitumor agents: molecular docking study', *Eur. J. Med.* **2010**, *45*, 4188–4198.
- [48] Q. Wang, H. Slegers, J. Clauwaert, 'Isolation of plasma membranes from rat C6 glioma cells cultivated on micro-carriers', *Acta Histochem.* **1999**, *101*, 327–339.
- [49] A. Pautsch, A. Zoephel, H. Ahorn, W. Spewak, R. Hauptmann, H. Nar, 'Crystal structure of bisphosphorylated IGF-1 receptor kinase: insight into domain movements upon kinase activation', *Structure* **2001**, *9*, 955–965.
- [50] D. Bhakta, R. Siva, 'Morindone, an anthraquinone, intercalates DNA sans toxicity: a spectroscopic and molecular modeling perspective', *Appl. Biochem. Biotechnol.* **2012**, *167*, 885–896.
- [51] M. Shweta, D. Rashmi, 'In-vitro ADME studies of TUG-891, a GPR-120 inhibitor using Swiss ADME predictor', *J. Drug Deliv. Ther.* **2019**, *9*, 266–369.
- [52] A. Bergamo, G. Sava, 'Ruthenium anticancer compounds: myths and realities of the emerging metal-based drugs', *Dalton Trans.* **2011**, *40*, 885–896.
- [53] C. G. Hartinger, M. A. Jakupec, S. Zorbas-Seifried, M. Groessl, A. Egger, W. Berger Zorbas, P. J. Dyson, B. K. Keppler, 'KP1019, a new redox-active anticancer agent- Preclinical development and results of a clinical phase I study in tumor patients', *Chem. Biodiversity* **2005**, *5*, 2140–2154.
- [54] M. K. Awad, M. R. Mustafa, M. M. Abo Elnga, 'Computational simulation of the molecular structure of some triazoles as inhibitors for the corrosion of metal surface', *J. Mol. Struct.: THEOCHEM* **2010**, *959*, 66–74.
- [55] K. Srivastava, A. Srivastava, P. Tandon, K. Sinha, J. Wang, 'Spectroscopic, quantum chemical calculation and molecular docking of dipfluzine', *J. Mol. Struct.* **2016**, *1125*, 751–762.
- [56] M. Bavadi, K. Niknam, O. Shahraki, 'Novel pyrrole derivatives bearing sulfonamide groups: Synthesis in vitro cytotoxicity evaluation, molecular docking and DFT study', *J. Mol. Struct.* **2017**, *1146*, 242–253.
- [57] T. K. Kuruville, J. C. Prasana, S. Muthu, J. George, S. A. Mathew, M. Bavadi, K. Niknam, O. Shahraki, 'Novel pyrrole derivatives bearing sulfonamide groups: Synthesis in vitro cytotoxicity evaluation, molecular docking and DFT study', *Spectrochim. Acta A* **2018**, *188*, 382–393.
- [58] J. B. Foresman, A. Frisch, 'Exploring Chemistry with Electronic Structure Methods', Pittsburg USA, Carnegie Office Park, 1996.

Received November 27, 2019

Accepted March 5, 2020